

A MODEL LAW FOR WAVE IMPACTS ON COASTAL STRUCTURES

by

C. Ramkema^{*}ABSTRACT

For the design of the storm surge barrier in the Eastern Scheldt, a study has been carried out on wave impacts against coastal and marine structures. First a review was made of relevant literature, including both wave impacts on coastal structures and slamming of sea-going vessels. From this, the so-called Bagnolds piston model emerged as most appropriate to describe the wave impacts caused by standing waves against protruding elements. This model was then further elaborated to include both adiabatic and isothermal compression of the air cushion and to allow for the compression of the water. Moreover, a model was developed to determine the spatial pressure distribution. Finally, experiments were performed, the results of which were in satisfactory agreement with the mathematical models. Based upon the results of these studies, a scaling law is presented here, from which the pressure magnitude and the time history of the impact in nature may be determined.

1 Scope of the Study

As part of the preliminary investigation for the development of the storm surge barrier in the Eastern Scheldt (Figure 1) tests were carried out to study the wave impacts on the sluice gates in this barrier. As a possible solution caissons placed on a rubble foundation were examined (Figure 2). Wave impacts induced by breaking waves were not observed here because of the relatively large foreshore depth; however, wave impacts might occur locally if the standing wave in front of the gate is impeded by protruding structural elements. Due to the specific shape of the structure, a volume of air is trapped between the protrusion and the rising water level which acts as a spring, resulting in a typical oscillating pattern of the impact pressure history. A literature study was made to find a suitable mathematical model which, after experimental verification, could be used for the conversion of these impacts to an impact in nature.

2 Review of Literature

The first effort to measure wave impacts on maritime structures was made by Stevenson [53] in Scerryvore Rocks 150 years ago. Until 1935 the measurements were performed with instruments unsuitable for these fast phenomena. The first excellent measurements with a high frequency range were executed in Dieppe by Rouville et al [49] and in a laboratory by Bagnold [5]. The development of mathematical wave impact and slamming models started with von Karman's model [31]. Because of the resemblance between the slamming phenomenon and the wave impact a historical review of investigations of both subjects is presented here, showing the relations between the various models (Figure 7).

The various mathematical models for wave impacts and slamming can be com-

* Project Engineer, Delft Hydraulics Laboratory, The Netherlands

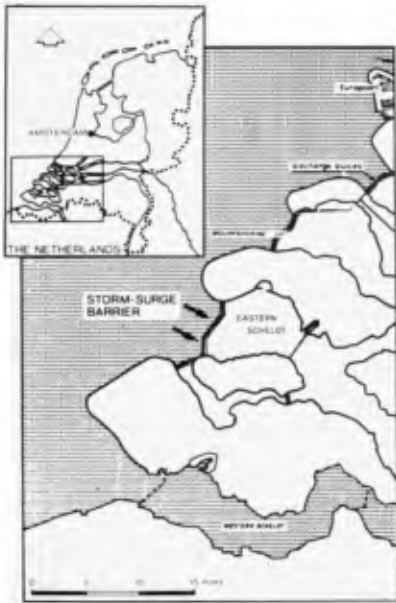


Fig. 1 Situation of the storm-surge barrier in the Eastern Scheldt

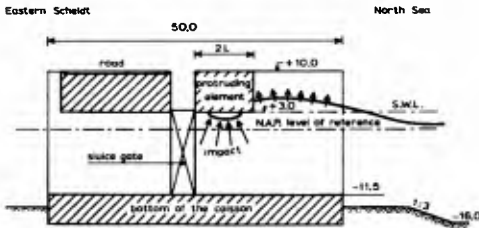


Fig. 2 Typical caisson-section for the storm-surge barrier (design 1975)

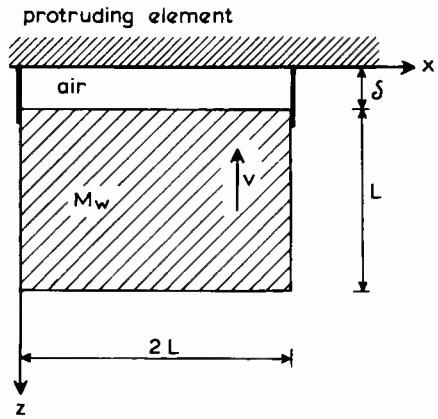


Fig. 4 The piston model of Bagnold

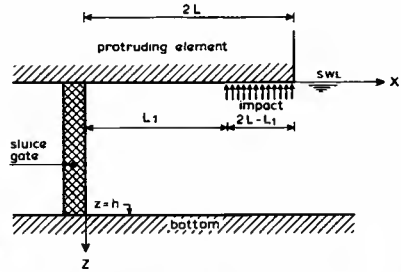


Fig. 5 Impact against the tip of the protrusion

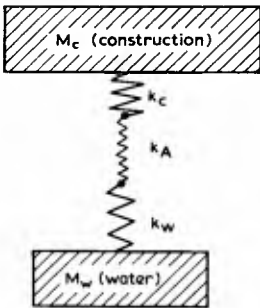


Fig. 3 The process schematized as a mass-spring system



Fig. 6 Impression of the instrumental equipment for the test

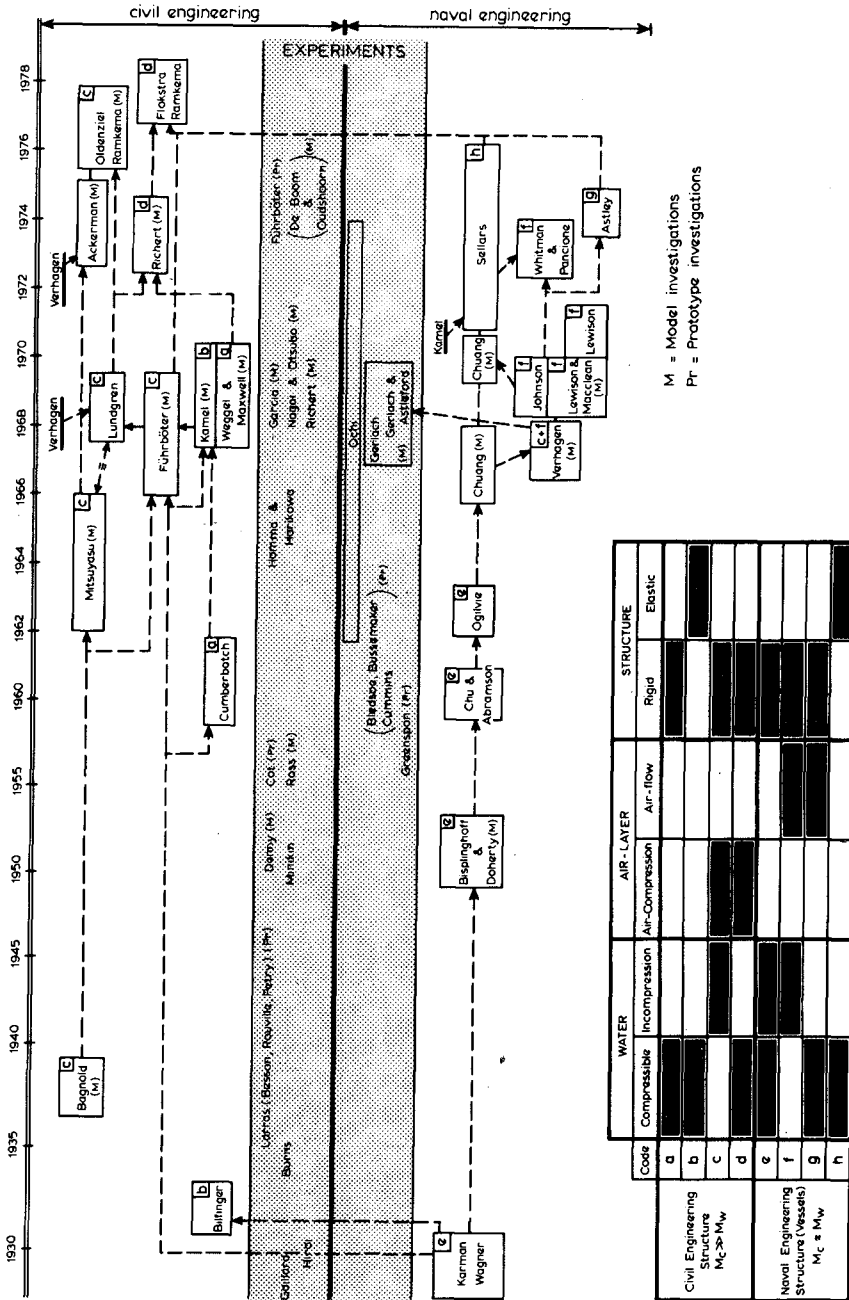


Fig. 7 Historical review of investigations on wave impact and slamming

bined into one general model (Figure 3), in which M_c is the mass of the construction; M_w is the equivalent hydraulic mass; and k_w , k_A and k_c are the spring constant of water, air and the construction respectively. For civil engineering constructions M_c is mostly much larger than M_w , whereas for ships and gates M_c and M_w are about equal.

The mathematical models in civil engineering can be divided into the way they take into account the importance of the compressed air layer with regard to the elasticity of the structure and the compressibility of water. Bagnolds model apparently is most appropriate to describe the impact against the protrusion, due to the specific air layer between the structure and the equivalent hydraulic mass.

The need for models in naval engineering first became apparent with the evident high pressures on V-shaped seaplane floats during landing. Later on, when the number of seaplanes decreased, impact pressures on high-speed ships stimulated research, as the calculated pressures on V-shaped wedges with the model developed by von Karman [31] were too conservative for these ships. Sellars [50,51] tried to explain the difference by accounting for the elasticity of the ship structure, whereas Verhagen [55] explains the difference by the elasticity of the air layer; the thickness of which is calculated by air flow between ship and water until the velocity of sound (C_A) is reached. For the subsequent stage he uses a Bagnold type piston model, with an air flow determined air layer thickness, for the determination of the impact pressure in which is accounted for the finite structure mass. However, the observed air layer between the caisson's protrusion and the water mass is mostly due to the specific shape of the protrusion and the water surface, so only the last part of Verhagen's model is appropriate for the description of our problem. Verhagen as well as Bagnold are supposing an adiabatic compression of the air layer.

Many experiments have been performed on civil and naval engineering structures, the results of which are generally expressed in the stagnation pressure: $\frac{1}{2} \rho v^2$, where ρ is the density of the water and v is the impact velocity. This is not further considered here, as in the impact process compressibility and air are certainly more important than the gravitational acceleration. Specially worth mentioning are the excellent experiments of Gerlach [21,22,23] in which the influence of liquid and gas properties and model shape on impact pressures of blunt rigid bodies is investigated. A more detailed literature description is in preparation by the author [44].

3 Theory

The observed air layer between the protruding element and the water mass gave evidence for the choice of Bagnold's piston model (in the tests $M_c \gg M_w$). Whether the compression of the air layer is adiabatic, isothermal or somewhere between depends upon such different factors as characteristic time of the phenomenon, the pressure magnitude, the air-water surface with regard to the air layer or bubble layer volume (the heat exchange by evaporation is much more important than by conductivity), the acceleration of the air-water surface and the irreversibility of the process. The significance of this question for model pressure conversion is evaluated in Paragraph 6.

Bagnold's model

The shape of the caisson and the protrusion is such that the phenomenon may be schematized as shown in Figure 4. A two-dimensional mass of water (M_w) with width $2L$ is travelling upward with a velocity v . For $z = \delta$ the

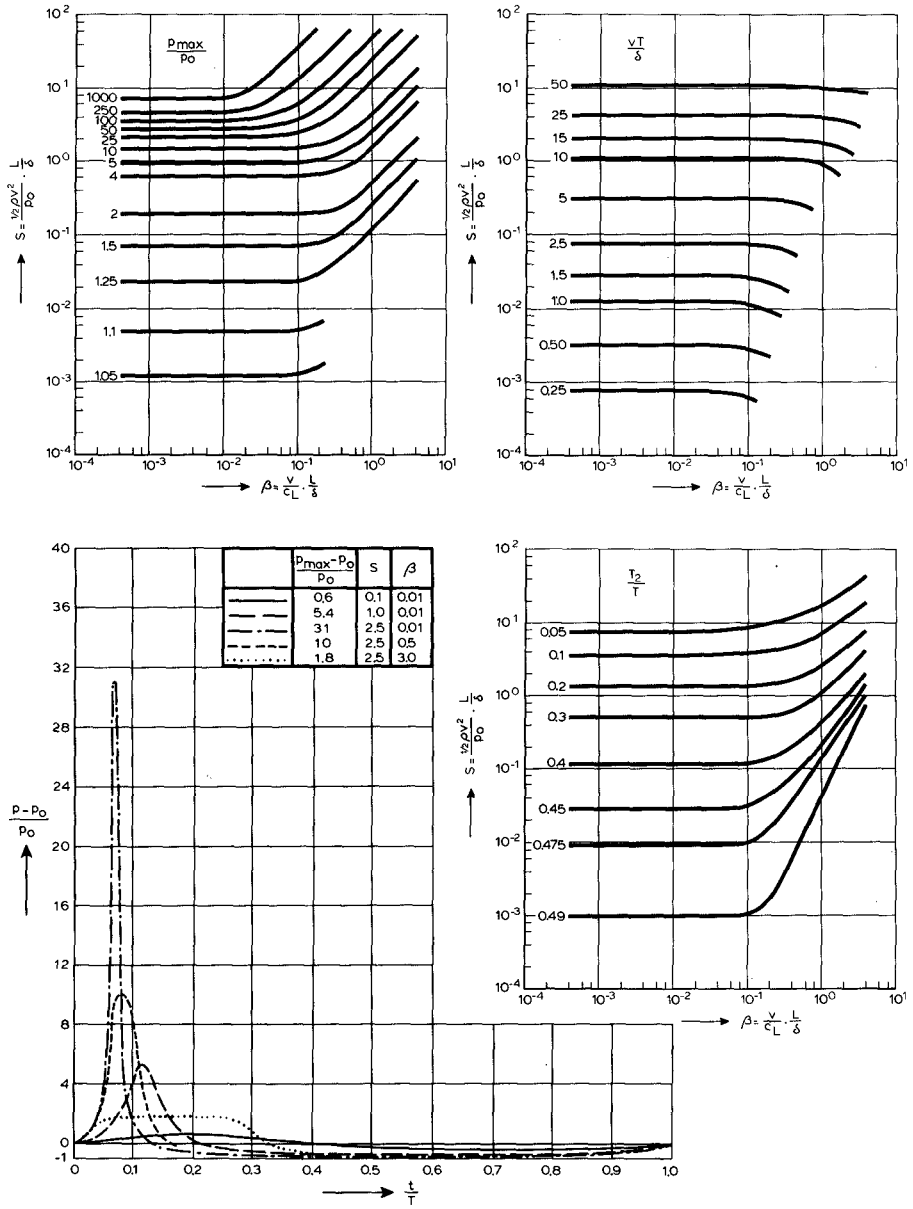


Fig. 8 Piston model with isothermal compression and compressible water: p_{max}/p_0 , $v T/\delta$ and T_2/T as a function of S and β

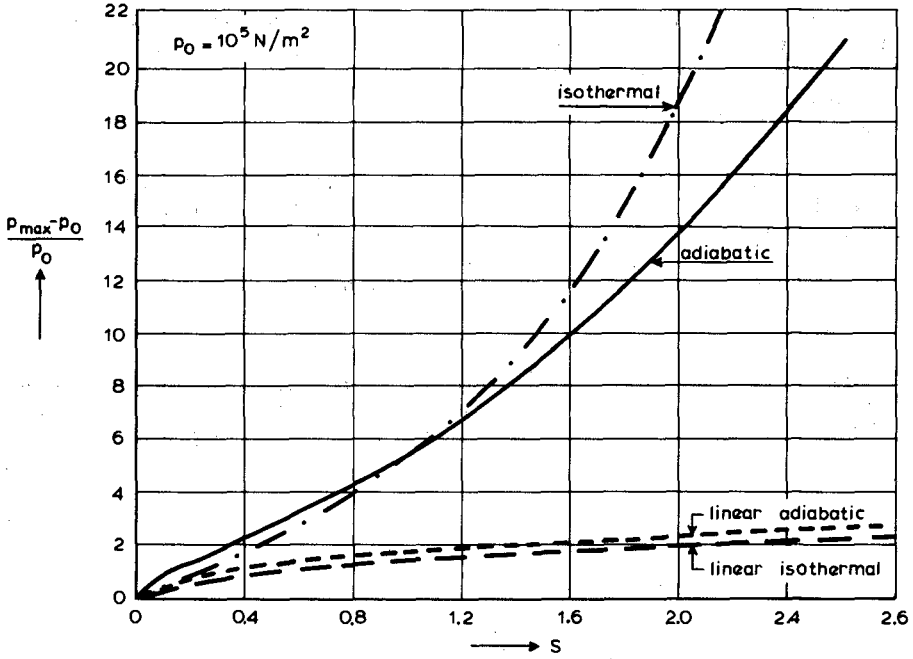


Fig. 9 Dimensionless peak pressure $(p_{max} - p_0)/p_0$ versus the impact number S for different compression models

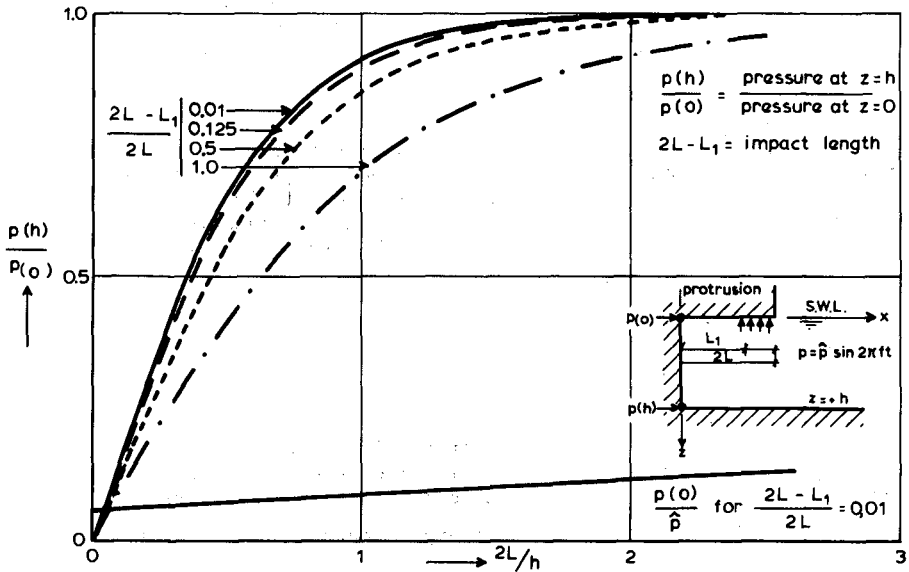


Fig. 10 Spatial distribution of the impact-pressure

air layer is blocked from the atmospheric pressure p_0 ; if the hydraulic mass of water per unit length is approximated by ρL^2 [58] the equation of motion can be written as:

$$M_w \frac{d^2 z}{dt^2} = p_2 L - p_0 L. \quad (1)$$

Here, forces due to the acceleration of gravity are neglected because in the time intervals under consideration the weight of the water mass will be small in general compared with the impact load. Moreover, the weight is compensated by the hydrostatic pressure.

The air compression is assumed to vary between adiabatic and isothermal, so:

$$p = p_0 \left(\frac{\delta}{z}\right)^\gamma, \quad (2)$$

where γ is the ratio between the specific heat at constant pressure and that at constant volume. For a linear compression, $|1 - z/\delta| \ll 1$, and with the initial conditions $z = \delta$ and $z = -v$, the following expressions can be derived for the maximum pressure:

$$p_{\max} = p_0 \left[1 + \sqrt{2 \gamma \frac{\frac{1}{2} \rho v^2 L}{p_0 \delta}} \right] = p_0 \left[1 + \sqrt{2 \gamma S} \right]. \quad (3)$$

The frequency of the oscillation is:

$$f = \frac{1}{2\pi} \sqrt{\frac{\gamma p_0}{\delta \rho L}}, \quad (4)$$

where S is defined as the impact number. The general solution for the dimensionless peak pressure $p_{\max} - p_0$, which satisfies Equations (1) and (2) with the mentioned initial conditions, is shown as a function of S in Figure 9. The graph for adiabatic compression is equivalent to Mitsuyasu's [38] and Lundgren's graph [36]. For a more detailed description of this derivation, see Ramkema et al [43].

Bagnold's model with compressible water

One of the basic criticisms of Bagnold's piston model is that for high impact numbers the pressure exceeds $\rho v c_w$ (where c_w is the velocity of sound in water). The one-dimensional mathematical model given below takes into account the compressibility of water. The impulse equation formulated in Lagrange coordinates with the centre on the air-water surface is:

$$\frac{\partial^2 z}{\partial t^2} \cdot \frac{\partial z}{\partial a} + \frac{1}{\rho} \frac{\partial p_w}{\partial a} = 0, \quad (5)$$

and the continuity equation is:

$$\rho \frac{\partial z}{\partial a} = \rho_0, \quad (6)$$

where a is the position of the water particles at $t=0$, ρ_0 is the local density of water at $t=0$, ρ is the local density of water, and p_w is the pressure distribution in the water column. After some rearrangements and the supposition that $\rho^2 \frac{\partial p_w}{\partial \rho}$ can be approximated with $\rho_0^2 c_w^2$, the equations can be written as:

$$\frac{\partial^2 z}{\partial t^2} - c_w^2 \frac{\partial^2 z}{\partial a^2} = 0, \quad (7)$$

with the initial conditions $z = a$ and $\frac{\partial z}{\partial t} = v$ for $-L < a < 0$ and the boundary conditions $p = p_0$ for $a = -L$ and $p_w = p$ (pressure in the air layer) for $a = 0$. The results of this piston model with compressible water are shown in Figure 8. The dimensionless maximum impact pressure p_{max}/p_0 , the dimensionless impact period $v T/\delta$, and the shape parameter T_2/T are given as a function of the impact number S and the compressibility number $\beta = v L/\delta c_w$; the ratio of the characteristic time interval for the impact pressure δ/v and the characteristic time interval for the compression wave L/c_w . For $\beta < 0.1$ and $S < 2$, compressibility of water can be neglected as can be seen from Figure 8. More detailed information is given in Ramkema et al [44].

Spatial pressure distribution

By supposing an homogeneous pressure field in the direction perpendicular to the draft (Figure 6), it is evident that for a wave impact against the whole length of the protruding structural element ($2L$) the pressure distribution over the gate will be almost uniform for large $2L/h$ values. For a small ratio $2L/h$, however, the pressure distribution over the gate will decrease exponentially with increasing z . To quantify this supposition, a mathematical model was used to describe the phenomenon [43]. Supposing a two-dimensional pressure field, zero viscosity, an irrotational motion and an incompressible fluid, this problem is solved by determining the following velocity potential ϕ which satisfies Laplace's equation and the boundary conditions:

$$\frac{\partial \phi}{\partial z} = 0 \text{ at } z = h, x > 0 \text{ and at } z = 0, 0 < x < L_1$$

$$\frac{\partial \phi}{\partial x} = 0 \text{ at } 0 < z < h, x = 0$$

$$p = p_m \cos 2\pi ft \text{ at } z = 0, L_1 < x < 2L.$$

The condition on the free surface ($z = 0$) is generally:

$$g \frac{\partial \phi}{\partial z} + \frac{\partial^2 \phi}{\partial t^2} = -\frac{1}{\rho} \frac{\partial \rho}{\partial t}, \quad (8)$$

where g is the gravitational acceleration. For high frequencies, $g \frac{\partial \phi}{\partial z}$ can be neglected with regard to $\frac{\partial^2 \phi}{\partial t^2}$. The ratio of the pressure amplitude at $z = h$ and at $z = 0$ is shown in Figure 10 as a function of $2L/h$ for different $(2L - L_1)/2L$ values.

4 Experimental Set-up

To verify the frequency behaviour of Bagnold's piston model and the spatial pressure distribution over the gate, a variety of tests has been made. The tests were performed with random waves in a $95 \times 0.90 \times 1.0 \text{ m}^3$ wind wave flume (Figure 11) provided with a flap-type wave generator. A scale model (1:50) was constructed from stainless steel (thickness 20 mm), representing a vertical face fronted by a rectangular protrusion with different lengths (figures 12 and 13). In this model wave impacts were measured at four locations to determine the frequency behaviour, and at six locations for the spatial pressure distribution. The unused holes were filled up with screw bolts flush with the front face of the wall. The wave impacts were measured with Statham PM 131TC pressure cells. The overall accuracy of the amplitude response of the total measuring system was about 90% for a frequency range of 0-2400 Hz. A general impression

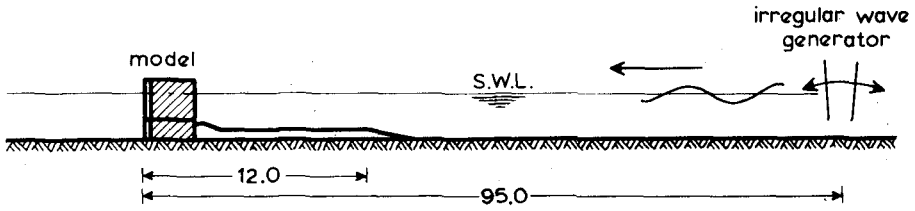


Fig. 11 Cross-section through wave channel

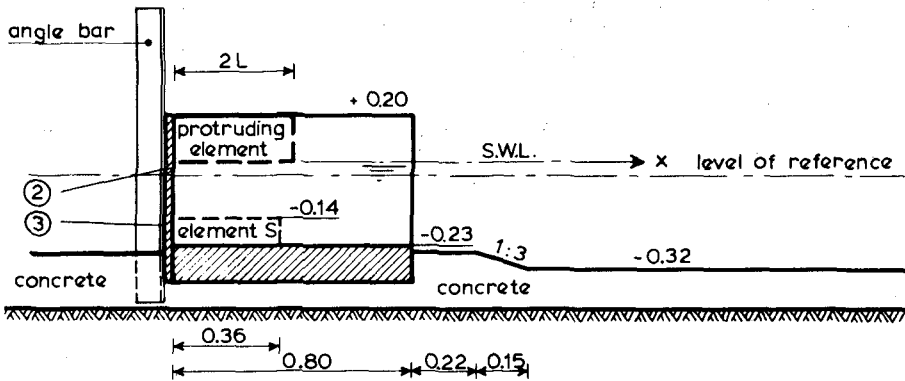


Fig. 12 Detail of test section

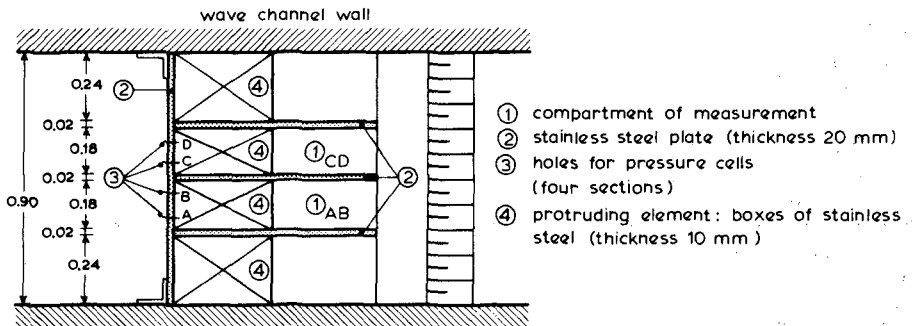


Fig. 13 Top view of test section

of the instrumental equipment for the tests is shown in Figure 6. The duration of each test was about 1000 zero crossing waves. However, the sensibility for wave impacts fluctuates strongly with the length of the protrusion and the water level with regard to the level of the protrusion. That is why the number of analysed impacts per test is not equal. Besides, only impacts $> 2000 \text{ N/m}^2$ were analysed. The tests for the spatial pressure distribution were limited to about 30 analysed wave impacts.

5 Experimental Results

In the investigation over 100 tests were made, a few of which had a geometry which could be used (see Tables 1 and 2) to test the given mathematical model. However, some general remarks based upon all the tests can be made:

- 1 The time history of the wave impact pressure can generally be described as a damped harmonic vibration. The impact frequency (f) is the reciprocal of the characteristic time of the vibration (Figure 14).
- 2 The impacts in the separated compartments AB and CD are uncorrelated for the frequency and the magnitude of the impact. However, the probability density functions for frequency and magnitude in the separated compartments are equal.
- 3 The pressure distribution in y-direction is about homogeneous in a compartment, with only a slight increase (about 10%) in the angles.
- 4 In general, the exceedance distribution for the impact pressure can be approximated, by a straight line, on logarithmic-linear paper. However, impacts smaller than 2000 N/m^2 are not taken into account (Figure 16).

To predict a maximum impact pressure it is necessary to know the maximum impact velocity, the minimum air layer thickness and the minimum protrusion length involved, but as a result of the mutual interactions this is extremely difficult. It is easier to predict the theoretical minimum impact frequency, which is a function of the maximum protrusion length involved and the maximum air layer thickness.

The impact frequency behaviour has been tested with four different lengths of the protruding element (Table 1). The analysed impacts did not exceed an impact pressure of $10,000 \text{ N/m}^2$ in model and the maximum air layer thickness could be visually estimated during the tests, being $1/10$ of the length of the protrusion. From each impact registration the impact pressure magnitude and the impact frequency were measured (Figure 15); the minimum and maximum value of the impact frequency are shown in the Table 1. With the visually estimated maximum air layer thickness and the length of the protrusion the theoretical minimum impact frequency can be calculated with Equation (4) for adiabatic ($\gamma = 1.4$) and isothermal compression ($\gamma = 1.0$). The linear approximation will be acceptable for impact pressures smaller than $10,000 \text{ N/m}^2$. The results of the comparison between the theoretical and the measured minimum impact frequency values is shown in Figure 18. It is evident that Bagnold's piston model is satisfactory for the prediction of the minimum impacts frequency, but whether the compression is adiabatic or isothermal cannot be concluded from this result.

The theory for the spatial pressure distribution over the gate was tested with the results of 7 tests carried out with 6 pressure cells, several of which were located in the protrusion. Depending upon the length $2L$, about 30 impacts of each test were analysed (as an example see Table 3 and Figure 17), and the coefficients, whose range is given in Table 2, were determined. The result of the comparison between the theoretical and the experimental maximum ratio p_B/p_{BB} is shown in Figure 19. As the theoretic-

test	protruding element		still water level (m)	wave conditions			positions of the pressure cells				frequency analysis			remarks
	length (m)	level (m)		reflection (%)	peak period (s)	significant wave height (m)	A (m)	B (m)	C (m)	D (m)	number of analysed impacts	minimum value of the frequency (s ⁻¹)	maximum value of the frequency (s ⁻¹)	
T 16	0.40	+ 0.06	+ 0.11	58	1.35	0.094	0	+ 0.04	- 0.02	+ 0.02	68	25	1050	compartment A, B compartment C, D wind velocity 4 m/s wind velocity 4 m/s
T 17	0.40	+ 0.06	+ 0.06	33	1.75	0.062	0	+ 0.04	- 0.02	+ 0.02	223	17	1550	
T 31	0.06	+ 0.06	+ 0.11	71	1.40	0.092	0	+ 0.04	- 0.02	+ 0.02	157	170	1250	
T 32	0.06	+ 0.06	+ 0.06	57	1.24	0.066	0	+ 0.04	- 0.02	+ 0.02	385 468	130 130	1650 1550	
T 39	0.06	+ 0.06	+ 0.11	73	1.39	0.084	0	+ 0.04	- 0.02	+ 0.02	46	130	1050	
T 40	0.06	+ 0.06	+ 0.06	57	1.23	0.068	0	+ 0.04	- 0.02	+ 0.02	278	120	1750	
T 49	0.18	+ 0.06	+ 0.11	67	1.40	0.096	0	+ 0.04	- 0.02	+ 0.02	170	38	400	
T 50	0.18	+ 0.06	+ 0.06	51	1.21	0.066	0	+ 0.04	- 0.02	+ 0.02	97	70	1750	
T 52	0.02	+ 0.06	+ 0.11	67	1.43	0.096	0	+ 0.04	- 0.02	+ 0.02	9	410	1600	
T 53	0.02	+ 0.06	+ 0.06	63	1.27	0.064	0	+ 0.04	- 0.02	+ 0.02	46	550	1800	

Table 1 Tests for frequency behaviour as a function of the length of the protruding element

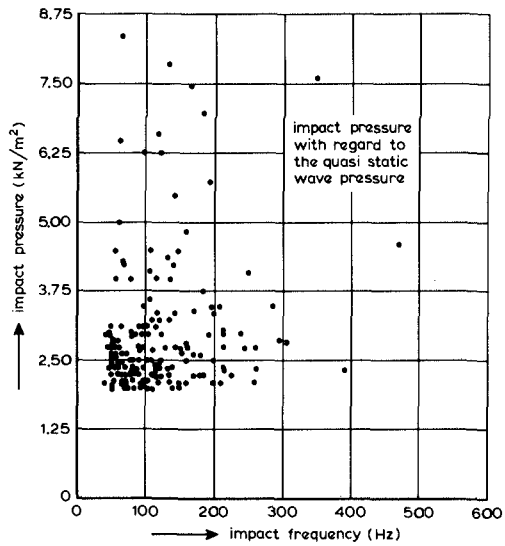


Fig. 15 Correlation between amplitude and frequency for impacts in compartment CD

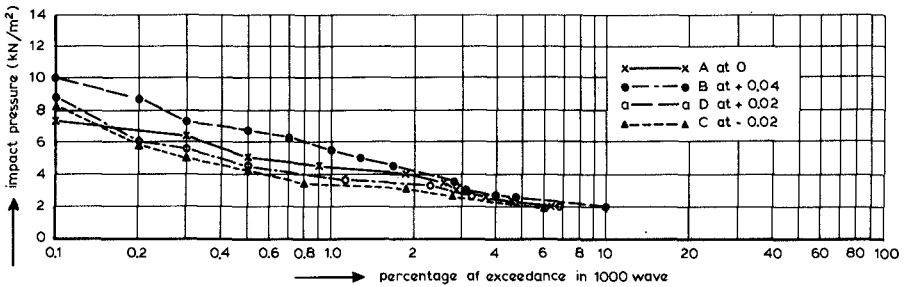
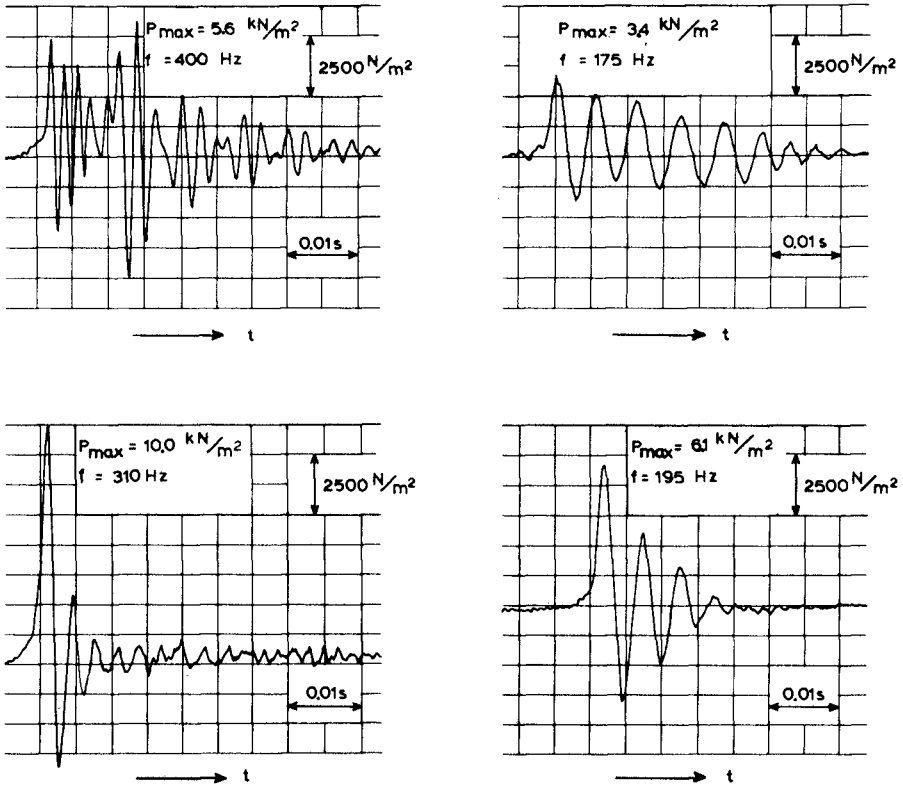


Fig. 16 T49: Exceedance distribution for wave impacts on the pressure cells: A, B, C and D



P_{max} : impact pressure with regard to the quasi static wave pressure

Fig. 14 T32: Typical impact-pressure recorded at 0.04 m above reference level (section B)

test	protruding element		special element S	still water level (m)	wave conditions			position of the pressure cells in compartment A & B						coefficient analysis			
	length (m)	level (m)			reflection (%)	peak period (s)	significant wave height (m)	compartment A & B						number of analysed impacts	2 L/h	minimum value of the coefficient	maximum value of the coefficient
								1	2	3	4	5	6				
T 91	0.70	+ 0.06		+ 0.06	51	1.20	0.082	+ 0.04	- 0.08	- 0.20	+ 0.06 (x = 0.05)	+ 0.05 (x = 0.25)	+ 0.06 (x = 0.65)	38	2.42	0.08	0.80
T 92	0.40	+ 0.06		+ 0.06	33	1.22	0.062	+ 0.04	- 0.08	- 0.20	+ 0.06 (x = 0.04)	+ 0.06 (x = 0.20)	+ 0.06 (x = 0.36)	40	1.38	0.07	0.80
T 93	0.18	+ 0.06		+ 0.06	51	1.27	0.070	+ 0.04	- 0.04	- 0.12	+ 0.06 (x = 0.06)	+ 0.06 (x = 0.14)	20	0.62	0.08	0.77	
T 94	0.04	+ 0.06		+ 0.06	57	1.22	0.072	+ 0.04	0	- 0.04	- 0.12 (x = 0.03)	+ 0.06 (x = 0.03)	35	0.207	0.05	0.35	
T 95	0.02	+ 0.06		+ 0.06	83	1.24	0.066	+ 0.04	0	- 0.04	- 0.08 (x = 0.03)	- 0.12 (x = 0.03)	25	0.069	0.03	0.18	
T 96	0.06	+ 0.06	x	+ 0.06	53	1.20	0.062	+ 0.04	0	- 0.04	- 0.08 (x = 0.03)	- 0.12 (x = 0.03)	26	0.30	0.11	0.42	
T 97	0.06	+ 0.02	x	+ 0.06	49	1.03	0.040	0	- 0.04	- 0.08	- 0.12 (x = 0.03)	-	32	0.375	0.10	0.56	

Table 2 Tests for spatial distribution behaviour as a function of 2L/h

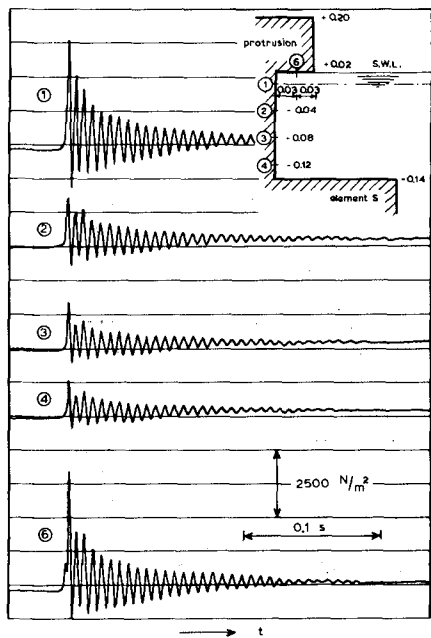


Fig. 17 T97: Typical simultaneous pressure recordings. Impact no. 21

impact no.	pressure on the pressure cells (mm)						frequency (s ⁻¹)	coefficient
	1	2	3	4	5	6		
1	20.5	10.5	8.0	7.0	24.5	150	0.34	
2	27.0	12.5	9.0	7.5	29.0	150	0.38	
3	33.0	14.5	14.5	11.5	47.5	200	0.35	
4	18.5	8.5	6.0	5.5	9.0	260	0.30	
5	14.5	9.0	7.0	6.0	17.0	160	0.41	
6	8.0	6.5	5.5	4.5	11.5	250	0.56	
7	29.0	14.0	10.0	8.5	36.0	150	0.29	
8	17.0	12.5	9.5	9.0	15.0	175	0.53	
9	25.0	14.0	11.0	9.5	31.0	180	0.38	
10	14.5	4.0	4.0	3.0	7.0	240	0.21	
11	10.0	3.0	3.0	2.0	7.0	220	0.20	
12	17.5	10.0	7.0	6.0	19.5	140	0.34	
13	12.0	5.5	4.0	4.0	16.5	200	0.33	
14	17.0	4.0	2.5	2.0	11.5	400	0.12	
15	22.5	12.0	9.0	7.5	26.0	140	0.33	
16	22.5	12.5	10.0	8.5	26.0	260	0.38	
17	19.5	4.5	3.0	2.0	6.0	1000	0.10	
18	21.0	11.5	8.0	7.0	23.0	130	0.33	
19	8.0	6.0	5.0	4.5	12.5	400	0.56	
20	22.5	10.0	7.5	6.0	17.0	160	0.27	
21	32.0	14.5	13.5	10.5	36.0	280	0.29	
22	12.5	9.0	7.0	6.5	14.5	640	0.52	
23	18.5	10.5	7.5	7.0	20.5	130	0.38	
24	14.5	6.5	4.5	3.5	20.5	180	0.24	
25	12.0	4.5	3.5	2.5	7.0	215	0.21	
26	18.5	8.0	6.5	5.0	14.5	190	0.27	
27	14.5	7.5	5.5	4.5	12.5	180	0.31	
28	39.0	24.0	18.5	16.0	46.5	150	0.41	
29	25.5	16.0	12.0	10.0	28.5	130	0.39	
30	24.0	12.0	8.5	8.0	28.0	130	0.33	
31	14.0	8.0	6.5	5.5	16.5	260	0.39	
32	8.5	4.5	3.0	2.0	12.0	240	0.24	

1 mm ≅ 125 N/m² with regard to the quasi static wave pressure

$$\text{coefficient} = \frac{\text{pressure on cell 4}}{\text{pressure on cell 1}}$$

Table 3 T97: Spatial pressure distribution of wave impacts

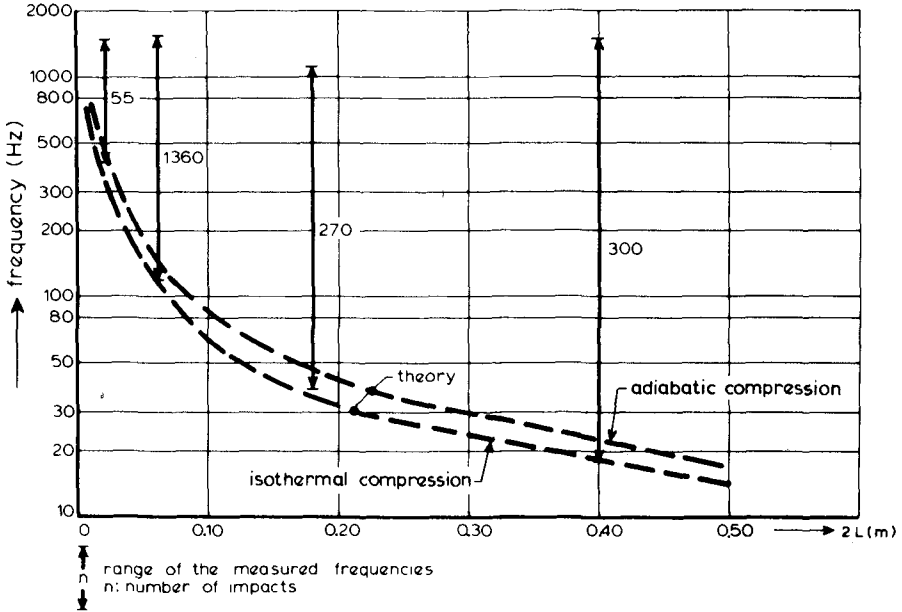


Fig. 18 Minimum frequencies as a function of the length of the protrusion ($2L$)

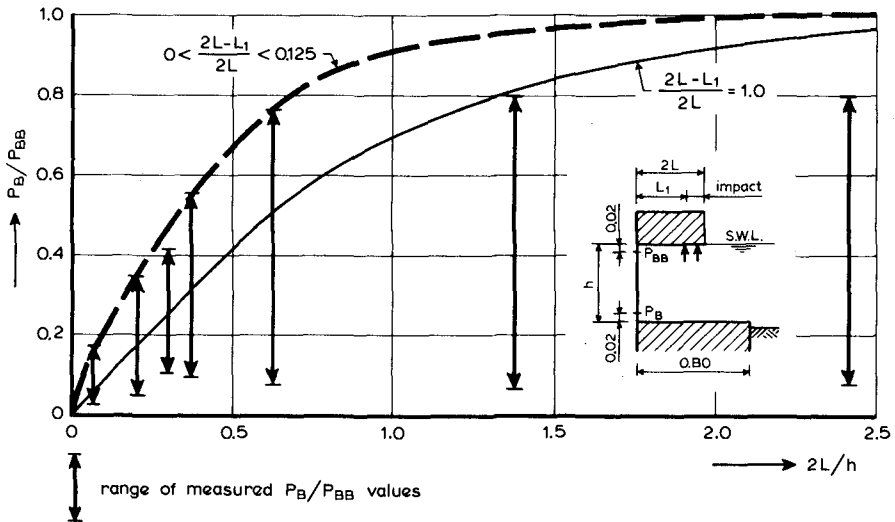


Fig. 19 Extreme spatial pressure distribution for $x = 0$, as a function of $2L/h$

cal curve hardly changes for $0 < \frac{2L - L_1}{2L} < 0.125$, only one curve has been drawn for these values. The second curve in this figure describes the situation in which the whole protrusion is struck by the standing wave, but this situation does not give the maximum coefficients. Due to the limited dimensions of the pressure cell, the mentioned ratio will be slightly larger than the theoretical $p(h)/p(o)$ ratio, but the comparison is still very satisfactory. However, for $2L/h > 1$, the experimental values are substantial smaller than the theoretical values. This was confirmed by the observations, where two impacts could be distinguished: one in front of the gate and a second at the end of the protrusion. The pressure on the gate as a result of this second impact was negligible and difficult to separate from the first. The results presented are spatial pressure distributions for impacts in front of the gate which, consequently, do not confirm the theoretical model.

6 Model Law

Although the agreement between the model experiments and the linear piston model was satisfactory, non-linear effects cannot be neglected for full-scale processes. Therefore the non-linear adiabatic and isothermal compression models have been elaborated (Paragraph 3). In order to use these mathematical models for the conversion of model-to-nature impact characteristics, the type of thermo-dynamic process, the influence of compressibility and the scaling factor of the impact-number S have to be determined. Because the shape of caisson and water surface is determinant for the air layer thickness and the hydraulic mass involved, the scaling factor for δ and L is linear ($n_\delta = n_L$; $n_v = n_L$). The external water movement obeys Froude's law, so $n_v = \sqrt{n_L}$ where the atmospheric pressure is equal in model and nature ($n_{p_0} = 1$). This results in a linear scale for the impact number S , or $n_S = n_L$. The thermodynamic similarity is difficult to evaluate. Due to the larger air volume and the higher pressure, the process in nature will be more adiabatic, whereas as a result of the larger air-water surface, the longer characteristic period and the state of the water surface the process in nature will be more isothermal than in model tests. However, in general the non-linear isothermal conversion is a little (10% for $p_{max} < 10 p_0$) more conservative, so this model was chosen. The influence of the compressibility can be evaluated with the compressibility number ($\beta = vL/\delta c_w$). For the model investigation $v < 1$ m/s, $2L < 0.40$ m and $c_w = 1540$ m/s; the minimum air layer thickness will be estimated with Verhagen's [55] first approximation for one-sided outflow $\delta = v \cdot 2L/c_A$, where c_A is the velocity of sound in air (≈ 340 m/s). So the compressibility number in model (1:50) has a maximum value of 0.11 and a minimum value, for $\delta = 1/10.2 L$, or 0.007. In nature this value will vary between 0.11 and 0.05. As can be seen from Figure 8, the influence of compressibility can be neglected, for $\beta < 0.1$ and $p_{max}/p_0 < 10$. The isothermal compression model law is presented in Figure 20 for $\beta < 0.1$ and $p_{max}/p_0 < 10$. If a similar time history of the impact in model and nature is supposed, the time scale can be related to the pressure scale if the total momentum obeys Froude's law. However, in general the full-scale time history is not similar to that in model due to the effect of the atmospheric pressure p_0 , which is equal in model and nature. Pressure amplitudes in model will generally be small with respect to the atmospheric pressure whereas in nature minimum values may approach zero pressure. Therefore the shape of the pressure fluctuation in full-scale may show sharp crests and flat troughs contrary to the sinusoidal fluctuation in model. Elaboration of the dimensionless fluctuation period vT/δ with Figure 21 shows that

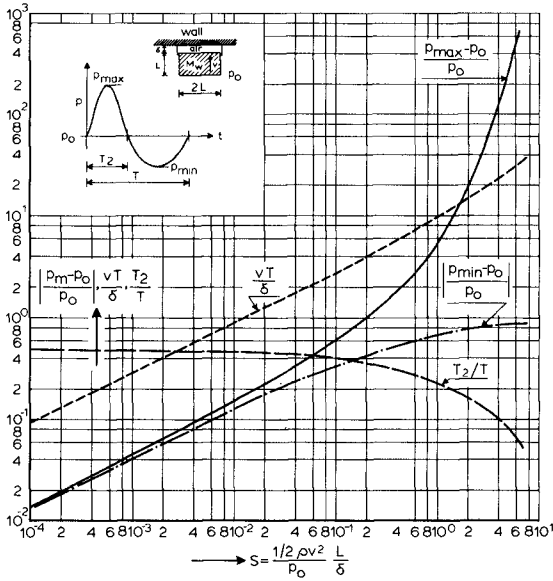


Fig. 20 Model-law for isothermal compression

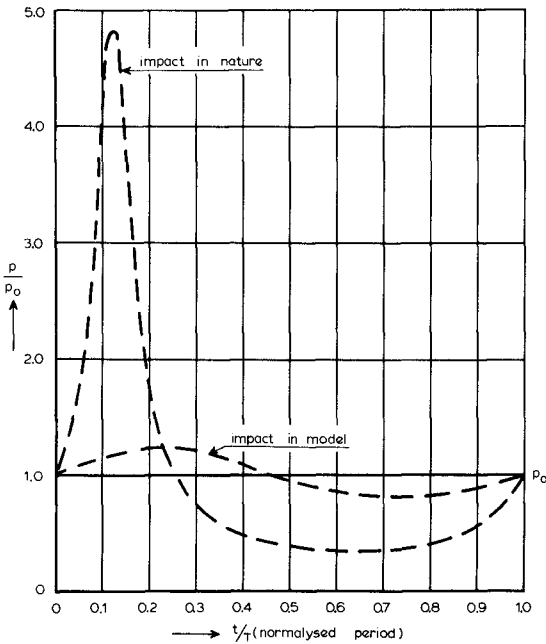


Fig. 21 Example of impact conversion

Example : impact conversion for a scalefactor 50

Model impact : $p_{max} - p_0 = 20 \text{ kN/m}^2$
 $f_{model} = 400 \text{ Hz}$

$$S_{model} = 0.015$$

length scalefactor : 50

$$S_{nature} = 0.75$$

Nature impact : $p_{max} - p_0 = 380 \text{ kN/m}^2$
 $p_{min} - p_0 = 65 \text{ kN/m}^2$
 $f = 8 \text{ Hz}$
 $T_2/T = 0.26$

$n_{yT}/\delta = n_S^{\frac{1}{2}}$ for practical impact pressures ($p_{\max} < 10 p_0$).

With the help of Figure 20, p_{\max} , p_{\min} , T_2/T and T of the given model impact pressure can be converted to an impact in nature. See as an example Figure 21 for $n_S = 50$.

The spatial pressure distribution over the gate in nature will be geometrically similar to the impact in model.

7 Discussion and Comments

As a result of the fact that the minimum impact frequency can well be predicted with Bagnold's linear piston model a non-linear isothermal compression model law is presented. The conversion of model impact pressures can easily be done with the help of Figure 20. However, it is questionable whether the described model law for an impinging standing wave against the protrusion is comparable, for example, with a breaking wave against a composite breakwater.

A striking feature of the described impact pressures was the damped oscillation, but this phenomenon was also seen by Bagnold [5], Mitsuyasu [38] Rouville et al [49], Ross [48], Gerlach [21], Chuang [12] and many others. The observed combination of an air layer and a maximum impact pressure at the same location was also observed in investigations from Richert [45], Ross [48], Gerlach [21], etc. However, the observed damping of impact pressures by breaking waves against breakwaters is much larger, which can be explained by the larger pressure radiation for flat structures like a breakwater front compared with the "hollow" structure used for the present tests. The conversion of a wave impact of breaking waves against a breakwater is dominated by the question: which part of the wave height (H) is involved in the process in nature compared with that in model? Supposing the breaking wave in a scale model ($M_C \gg M_w$) has all the features (geometrical and kinematic) of the wave in nature, then the wave height involved is on a linear scale and so is the thickness of the air layer resulting from the concave part of the breaking wave front. At the limit (but hardly imaginable) the thickness of the air layer is determined by the air flow (see Verhagen [55]). The flatness of the water surface (parallel to the breakwater front) required for this air flow process, however, has a very low probability of occurrence, especially in breaking wave fronts and has therefore been neglected. So the scale factor for the impact number S is n_1 , under the supposition of a linear scale for the involved wave height and the air layer thickness. The measured impact on the breakwater model can now be converted to an impact in nature as far as peak pressure, characteristic time and shape of the impact are concerned. With the help of Weggels' or Richert's mathematical model, or with the model presented here with modified boundary conditions, the spatial pressure distribution can be calculated. The response function of the structure will finally determine the response to this impact force.

Acknowledgements

The Author wishes to thank the Hoofdafdeling Waterloopkunde of the Delta-dienst of the Rijkswaterstaat for permission to publish the results of the investigation.

NOTATION

a	positions of the water particles at $t = 0$	p	pressure in the air layer
c_A	velocity of sound in air	p_0	atmospheric pressure (100,000 N/m ²)
c_w	velocity of sound in water	p_m	extreme pressure in the air layer
f	frequency of the pressure oscillation (1/T)	p_w	pressure in the water column
g	gravitational acceleration	S	impact number $\frac{1}{2} \frac{\rho v^2}{p_0} \cdot \frac{L}{\delta}$
h	distance between the protruding element and the bottom	t	time
k_A	"spring constant" of air	T	period of the impact pressure oscillation
k_C	"spring constant" of the construction	T_2	peak time of the impact pressure oscillation
k_w	"spring constant" of water	v	velocity of the water mass
L	length of the water column	z, x	vertical and horizontal coordinate
L_1	part of the protruding element (Figure 19)	β	water compressibility number $\frac{v}{c_w} \cdot \frac{L}{\delta}$
2 L	length of the protruding element	γ	ratio between the specific heat at constant pressure and that at constant volume
M_C	mass of the structure	δ	thickness of the air layer
M_w	equivalent hydraulic mass	ρ	density of water
n_i	scale factor of parameter i	ϕ	velocity potential
n_l	scale factor of length		

REFERENCES

- 1 AARTSEN, M.A. and VENIS, W.A., Model investigations on Wave Attack on Structures, IAHR 8th Congress, Montreal, Aug. 24-29, Vol. 1, 1959
- 2 ACKERMAN, N.L., Impact pressures produced by breaking waves, Procs. Coastal Engineering Conference, Copenhagen, Chap. 104, 1974
- 3 ASTLEY, R.J., An idealised model for flat-bottomed ship slamming, Procs. Fifth Australian Conference on Hydraulics and Fluid Mechanics, Vol. II, 1974
- 4 BAKER, W.E., WESTINE, P.S., GARZA, L.R., and HUNTER, P.A., Water Impact Studies of Model Apollo Command Module, Appendix A, Impact Simulation, Final Report, Southwest Research Institute, Project No. O2-1541, Aug. 1965
- 5 BAGNOLD, R.A., Interim report on wave pressure research, Journal of the Institution of Civil Engineers, London, Vol. 12, June 1939
- 6 BILFINGER, W., Molenbau und Wellenwirkung, Thesis presented to the Technischen Hochschule München, 1934
- 7 BISPLINGHOFF, R.L., and DOHERTY, C.S., Some Studies of the Impact of Vee Wedges on a Water Surface, Journal of the Franklin Institute, Vol. 153, 1952
- 8 BOOM, J. de en OUDSHOORN, B., Onderzoek naar de invloed van de dichtheid en de compressibiliteit van lucht op golfklappen, Afstudeerverslag Technische Hogeschool Delft, 1976
- 9 BRUNS, E. (1951), Berechnung des Wellenstosses auf Molen und Wellenbrecher, Jahrbuch der Hafenbautechnischen Gesellschaft, 9. Band, 1941-1949, Berlin, 1951
- 10 CHU, WEN-WHA and ABRAMSON, H.N., Hydrodynamic Theories of Ship Slamming - Review and Extension, Journal of Ship Research, Vol. 4, No. 4, Marz 1961
- 11 CHUANG, S.L., Investigation of Impact of Rigid and Elastic Bodies with water, Naval ship Research and Development Center, Report 3248, Febr. 1970
- 12 CHUANG, S.L., Experiments on slamming of Wedge-Shaped Bodies, Journal of Ship Research, Sept. 1967

- 13 COT, P.D., Le Laboratoire du Havre pour la mesure des efforts dus aux lames, Procs. Coastal Engineering Conference, Chap. 40, 1954
- 14 CUMBERBATCH, E., The Impact of a Water Wedge on a Wall, Journal of Fluid Mechanics, Vol. 7, Part 3, 1960
- 15 DENNY, D.F., Further Experiments on Wave Pressure, Journal of the Institution of Civil Engineers, Vol. 35, June 1951
- 16 FUHRBOTER, A. (1966), Der Druckschlag durch Brecher auf Deichböschung-
gen, Mitteilungen des Franzius-Instituts für Grund- und Wasserbau der
Technischen Hochschule Hannover, Heft 28, 1966
- 17 FUHRBOTER, A., Laboratory investigations of impact forces, Procs. Re-
search on wave action, Vol. II, Delft, 1969
- 18 FUHRBOTER, A., Zufalls Prozesse bei der Belastung durch brechende
Wellen, Technischen Universität: Jahresbericht des Sonderforschungs-
bereichs 79: 4, Hannover, 1973; Teilprojekt C. Deutscher Forschungsge-
meinschaft, 1974
- 19 GAILLARD, D.D., Wave action in relation to engineering structures,
The Engineer School, U.S. Army Corps of Engineers, Ft. Belvoir, 1935
- 20 GARCIA, W.J., An experimental study of breaking-wave pressures, U.S.
Army Engineer Waterways Experiment Station, Research report H-68-1,
Sept. 1968
- 21 GERLACH, C.R., Investigation of Water Impact of Blunt Rigid Bodies -
Real Fluid Effects, Technical Report No. 1, Southwest Research In-
stitute Project No. 02-2036, Dec. 1967
- 22 GERLACH, C.R., Investigation of Water Impact of Blunt Rigid Bodies -
Size Scale Effects, Technical Report No. 2, Southwest Research In-
stitute Project No. 02-2036, Nov. 1968
- 23 GERLACH, C.R., and ASTLEFORD, W.J., Investigation of Water Impact of
Blunt Bodies, Final Report, Southwest Research Institute Project No.
02-2036, Dec. 1970
- 24 GREENSPON, J.F., Sea Tests of the U.S.C.G.C. Unimak Part 3 - Pres-
sures, Strains, and Deflections of the Bottom Plating Incident to
Slamming, NSRDC Report 978, Marz 1956
- 25 HAYASHI, T., and HATTORI, M., Pressure of the Breaker Against a Ver-
tical Wall, Coastal Engineering in Japan, Vol. 1, Tokyo, 1958
- 26 HIROI, I., The Force and Power of Waves, The Engineer, Vol. 130,
Aug. 1920
- 27 HOM-MA, M., and HORIKAWA, K., Wave Forces Against Sea Wall, Proc.
Ninth Conference on Coastal Engineering, Lisbon, June 1964
- 28 HOM-MA, M., and HORIKAWA, K., Experimental Study on Total Wave Forces
Against Sea Wall, Coastal Engineering in Japan, Vol. 8, Tokyo, 1965
- 29 JOHNSON, R.S., The effect of air compressibility in a first approxi-
mation to the ship slamming problem, Journal of Ship Research, Vol.
12, No. 1, Marz 1968
- 30 KAMEL, A.M., Shock Pressure on Coastal Structures, ASCE Journal of
the Waterways, Harbors and Coastal Engineering Div., Vol. 96, No. WW3,
Aug. 1970
- 31 Von KARMAN, T., The Impact on Seaplane Floats During Landing, Natio-
nal Advisory Committee for Aeronautics, TN 321, Washington D.C., 1929
- 32 LARRAS, J., Le Déferlement des lames sur les jetées verticales, Anna-
les Ponts et Chaussées, 1937
- 33 LEWISON, G., and MacLEAN, W.M., On the Cushioning of Water Impact by
Entrapped Air, Journal of Ship Research, Vol. 12, no. 2, June 1968
- 34 LEWISON, G., Slamming, Ship Division Report 138, National Physical
Laboratory, Marz 1970
- 35 LEWISON, G., On the Reduction of Slamming Pressures, Transactions,
RINA, Vol. 112, 1970

- 36 LUNDGREN, H., (1969), Wave Shock Forces: An Analysis of Deformations and Forces in the Wave and in the Foundation, Procs. Research on Wave Action, Vol. II, Delft, 1969
- 37 MINIKIN, R.R., Winds, Waves and Maritime Structures, London, 1950
- 38 MITSUYASU, H., (1966), Shock Pressure of Breaking Wave, Procs. Coastal Engineering Conference, Vol. 1, Tokyo, Sept. 1966
- 39 MITSUYASU, H., Shock pressure of breaking waves, Coastal Engineering in Japan, Vol. 9, Tokyo, 1966
- 40 NAGAI, S. en OTSUBO, T., Pressures by breaking waves on composite-type breakwaters, Procs. Coastal Engineering Conference, London, Sept. 1968
- 41 OCHI, M.K. and MOTTER, L.E., Prediction of Slamming Characteristics and Hull Responses for Ship Design, The Society of naval architects and marine Engineers, Transactions, Vol. 81, 1973
- 42 OGILVIE, T.F., Compressibility effects in ship slamming, Schiffstechnik, Band 10, Heft 53, 1963
- 43 RAMKEMA, C., FLOKSTRA, C., and OLDENZIEL, D.M., and WATERLOOPKUNDIG LABORATORIUM, Golfklappen op de schuif in de Oosterschelde-Caisson, Verslag M 1335 deel I, band 1, April 1977
- 44 RAMKEMA, C., and FLOKSTRA, C., and WATERLOOPKUNDIG LABORATORIUM, Golfklappen; Een literatuuroverzicht en de invloed van de samendrukbaarheid van het water, verslag M 1335 deel II, (in preparation)
- 45 RICHERT, G., Experimental Investigation of Shock Pressures Against Breakwaters, Procs. Coastal Engineering Conference, Vol. II, London, Sept. 1968
- 46 RIGHERT, G., Model Law for shock pressures against breakwaters, Paper 55, Coastal Engineering Conference, London, Sept. 1968
- 47 RIGHERT, G., Shock pressures of breaking waves, Hydraulics Laboratory, Royal Institute of Technology, Stockholm, Bulletin No. 84, 1974
- 48 ROSS, C.W., Laboratory Study of Shock Pressures of Breaking Waves, Beach Erosion Board, Dept. of the Army, Corps of Engineers, Tech. Memo, No. 59, Washington, Feb. 1955
- 49 ROUVILLE, L.M.A. de, BESSON, P. et PETRY, P., Etat actuel des études internationales sur les efforts dus aux lames, Annales des Ponts et Chaussées, VII, Paris, 1938
- 50 SELLARS, F., Slamming Impact Pressure, MPR Associates Report MPR-282, June 1971
- 51 SELLARS, F., Water impact loads, Marine Technology, Vol. 13, No. 1, Jan. 1976
- 52 SKLADNEV, M.F. en POPOV, I.Y., Studies of wave loads on concrete slope protections of earth dams, Procs. Research on wave action, Vol. II, Delft, 1969
- 53 STEVENSON, T., The Design and Construction of Harbours, Edinburgh, 1874
- 54 VENIS, W.A. (1960), Determination of the Wave Attack Anticipated Upon a Structure from Laboratory and Field Observations, Procs. Coastal Engineering Conference, Vol. 2, The Hague, Aug. 1960
- 55 VERHAGEN, J.H.G., The Impact of a Flat Plate on a Water Surface, Journal of Ship Research, Vol. 11, No. 4, Dec. 1967
- 56 WAGNER, H., Über die Landung von Seeflugzeugen, Zeitschrift für Flugtechnik und Motorluftschiffahrt, Band 22, 1931
- 57 WEGGEL, J.R., and MAXWELL, W.H.C. (1970), Numerical Model for Wave Pressure Distributions, ASCE Journal of the Waterways, Harbors and Coastal Engineering Division, Vol. 96, No. WW3, Aug. 1970
- 58 WESTERGAARD, H.M., Water Pressures on Dams During Earthquakes, Transactions of the ASCE, Vol. 98, Paper No. 1835, 1933
- 60 WHITMAN, A.M., and PANCIONE, M.C., A Similitude Relation for Flat-Plate Hydrodynamic Impact, Journal of Ship Research, Vol. 17, No. 1, Marz 1973